Limnol. Oceanogr., 55(1), 2010, 115–133
© 2010, by the American Society of Limnology and Oceanography, Inc.

Variability in greenhouse gas emissions from permafrost thaw ponds

Isabelle Laurion[a,b,*] Warwick F. Vincent,[b,c] Sally MacIntyre,[d] Leira Retamal,[a,b] Christiane Dupont,[a,b] Pierre Francus,[a,b] and Reinhard Pienitz[b,e]

[a] Institut national de la recherche scientifique, Centre Eau, Terre et Environnement, Québec, Québec, Canada
[b] Centre d'études nordiques, Université Laval, Québec, Québec, Canada
[c] Département de Biologie, Université Laval, Québec, Québec, Canada
[d] Marine Science Institute, University of California, Santa Barbara, California
[e] Département de Géographie, Université Laval, Québec, Québec, Canada

Abstract

Arctic climate change is leading to accelerated melting of permafrost and the mobilization of soil organic carbon pools that have accumulated over thousands of years. Photochemical and microbial transformation will liberate a fraction of this carbon to the atmosphere in the form of CO_2 and CH_4. We quantified these fluxes in a series of permafrost thaw ponds in the Canadian Subarctic and Arctic and further investigated how optical properties of the carbon pool, the type of microbial assemblages, and light and mixing regimes influenced the rate of gas release. Most ponds were supersaturated in CO_2 and all of them in CH_4. Gas fluxes as estimated from dissolved gas concentrations using a wind-based model varied from -20.5 to 114.4 mmol CO_2 m^{-2} d^{-1}, with negative fluxes recorded in arctic ponds colonized by benthic microbial mats, and from 0.03 to 5.62 mmol CH_4 m^{-2} d^{-1}. From a time series set of measurements in a subarctic pond over 8 d, calculated gas fluxes were on average 40% higher when using a newly derived equation for the gas transfer coefficient developed from eddy covariance measurements. The daily variation in gas fluxes was highly dependent on mixed layer dynamics. At the seasonal timescale, persistent thermal stratification and gas buildup at depth indicated that autumnal overturn is a critically important period for greenhouse gas emissions from subarctic ponds. These results underscore the increasingly important contribution of permafrost thaw ponds to greenhouse gas emissions and the need to account for local and regional variability in their limnological properties for global estimates.

The warming of subarctic and arctic regions is accompanied by permafrost melting and erosion and the production of numerous small basins that fill with water. These thaw (or thermokarst) lakes and ponds persist from days to hundreds of years depending on local geomorphology, climate, and hydrology (Åkerman and Malmström 1986; Pienitz et al. 2008). They are usually surrounded by peaty soils and vegetation and are therefore often rich in organic matter that will be partly mineralized and transferred to the atmosphere in the form of CO_2 and CH_4, two potent greenhouse gases (GHG). Thaw ponds need to be taken into account in global atmospheric carbon budgets and climate warming prediction models since they are significant sources of methane (Walter et al. 2006). These aquatic systems may contribute a positive feedback to climate warming (Schuur et al. 2008) and be partly responsible for the increase in global atmospheric CH_4 during the last deglaciation (Walter et al. 2007).

In general, small lakes and ponds represent a net source of CO_2 to the atmosphere (Sobek et al. 2005), and they are now recognized as important contributors to regional and global climate (Cole et al. 2007). Specific studies on thaw pond carbon cycling are scarce, but they all report a large evasion and/or a supersaturation of GHG in these systems (Hamilton et al. 1994 in the Hudson Bay region, Canada; Ström and Christensen 2007 in Scandinavia; Blodau et al. 2008 in Siberia). Several studies have considered how changes in the surface area covered by thermokarst systems could substantially alter the effect of high-latitude ecosystems on the atmosphere (Chapin et al. 2000). During a thaw–freeze cycle associated with thermokarst lake migration in Siberia, ~ 30% of yedoma carbon was apparently decomposed by microbes, converted to methane, and released to the atmosphere (Zimov et al. 1997). Recently, Walter et al. (2006) attributed a 58% increase in CH_4 emission in northern Siberia to the expansion of thaw lakes between 1974 and 2000.

The rate at which GHG are liberated to the atmosphere partly depends on the physical structure of the water column, which influences the light, temperature, and oxygen content, and thus the microbial assemblages and metabolic pathways. For example, Kankaala et al. (2006) showed in a boreal lake that 80% of CH_4 diffused from the sediment was consumed by methanotrophs and 20% was released to the atmosphere, proportions that were highly dependent on water column mixing. GHG efflux will also depend on the availability of dissolved compounds for microbial degradation and their reactivity to photolysis and on the activity of primary producers that will determine the metabolic balance of these shallow water ecosystems. Thus, several factors controlled by climate (temperature, water column stability, allochthonous inputs) have the potential to affect the contribution of small polar lakes to the atmospheric carbon budget (Vincent 2009).

Large differences in carbon evasion rates have been observed in different permafrost regions, especially for CH_4 evasion; however, little is known about the causes of this variability and how climate change may influence GHG production in the future. For terrestrial and wetland

* Corresponding author: isabelle.laurion@ete.inrs.ca

systems in permafrost regions, a complex set of variables has been suggested to control CH_4 emissions, including soil temperature, near-surface turbulence and atmospheric pressure, ground temperature and thaw depth, water table position, substrate availability to methanogens, and primary production (Sachs et al. 2008). Thaw lakes and ponds are a major, yet overlooked, class of aquatic ecosystems in polar regions (Pienitz et al. 2008).

Permafrost thaw ponds in northeastern Canada present a broad range of limnological properties that potentially influence their greenhouse gas production (Breton et al. 2009). The objectives of the present study were to measure gas exchange and to examine its controlling factors in thaw ponds of the Canadian Subarctic and Arctic. These two regions differ in that permafrost is continuous in the Arctic but discontinuous in the Subarctic, which leads to limnological differences in their aquatic ecosystems. We examined spatial variability by sampling 30 subarctic ponds and 22 arctic ponds, and temporal variability via repeated measurements in 12 ponds over two summers. Additionally, we conducted an intensive weeklong study at one site with continuous measurements of gas concentrations in the surface water and meteorological variables in the overlying atmosphere. We used the latter data set to compare three gas transfer models for estimating GHG exchange.

Methods

Study sites—Field sampling was from 21 to 27 July 2006 and from 28 June to 24 July 2007 at two contrasting sites (Fig. 1). Thirty of the study ponds were located in Nunavik (12 of these ponds were resampled in 2007) in the subarctic discontinuous permafrost region at 55°16′N, 77°46′W, near the village of Whapmagoostui-Kuujjuarapik (named KWK ponds hereafter). Another 22 ponds were sampled in 2007 in Sirmilik National Park, Bylot Island, Nunavut, in the arctic continuous permafrost region at 73°09′N, 79°58′W, near the village of Pond Inlet (named BYL ponds hereafter) (Table 1). The subarctic thaw ponds (Fig. 2a,b) are surrounded by dense shrubs (*Betula glandulosa*, *Salix* sp., *Alnus* sp., *Myrica gale*) and sparse trees (*Picea mariana*, *Picea glauca*, *Larix laricina*), with some areas colonized by *Sphagnum* spp. mosses. These thermokarst ponds are formed in depressions (1–3-m deep) left after the ice has melted below mineral mounds.

In the continuous permafrost area, the ponds are formed on low-center polygons and in runnels over melting ice wedges (or runnel ponds) at the surface of permafrost terrain (Fig. 2c,d). These ponds are a natural phenomenon associated with the active layer dynamics of organic soils but are likely increasing in importance with the accelerated warming and melting of permafrost (Schuur et al. 2008). At this site, there was a ca. 2.5-m thick peaty silt unit in the center of polygons, consisting of fibrous peat mixed with wind-blown sediment that originated from the nearby glaciofluvial outwash plain (Fig. 2e; *see* Fortier and Allard 2004 for geomorphological details). The active layer in this region is about 40-cm deep in the peaty silts. Four larger waterbodies were sampled for comparison: BYL36 is a large pond about 5.5-m deep that was considered in the same class as the other thaw ponds for averages (Fig. 2d); BYL37 is a kettle lake located next to the camp; and BYL39 and BYL40 are two oligotrophic lakes with a rock floor and located in a nearby valley in the proximity of alpine glaciers.

Physicochemistry—Temperature, dissolved oxygen, and pH were recorded with a 600R multiparametric probe (Yellow Spring Instrument). The oxygen probe was calibrated at the beginning of each sampling day in water-saturated air with a correction for barometric pressure. The temperatures at the surface (0.15 m) and bottom (2.0 m; max. depth ~ 2.2 m) of pond KWK16 were measured continuously from July 2007 through July 2008 with readings recorded every half hour (HOBOware™ U12 thermistors, Onset). Water samples were filtered through prerinsed cellulose acetate filters (0.2-μm pore size; Advantec Micro Filtration Systems) to measure the optical properties of dissolved organic matter (DOM). Dissolved organic carbon (DOC) concentrations were measured using a Shimadzu TOC-5000A carbon analyzer calibrated with potassium biphthalate. To determine the chromophoric fraction of DOM (CDOM), absorbance scans were performed from 250 to 800 nm on a spectrophotometer (Cary 100, Varian) at a speed of 240 nm min^{-1} and a slit width of 2 nm. Total phosphorus (TP) was measured by spectrophotometry as in Stainton et al. (1977) on unfiltered water samples fixed with H_2SO_4 (0.15% final concentration) and digested with potassium persulfate. The total suspended solids (TSS) were collected onto precombusted and preweighed glass fiber filters (0.7-μm nominal pore size; Advantec MFS) that were dried for 2 h at 60°C.

Meteorology—Meteorological variables were measured by nearby automated climate stations. At the arctic site, the climate station was up to 10 km from the sampled ponds (in three cases), but in most cases it was < 500 m. At the subarctic site, the station was installed beside pond KWK2, and up to 370 m from the furthest sampled pond at this site. Incident shortwave radiation (300–1100 nm, W m^{-2}), air temperature, relative humidity, and wind speed (m s^{-1}) were measured at 2 m aboveground and recorded every 30 min (WeatherHawk 511).

Bacteria and chlorophyll a—Water samples for bacterial abundance were fixed with a filtered solution of paraformaldehyde (1% final concentration) and glutaraldehyde (0.1% final concentration) after adding a protease inhibitor (phenylmethanesulphonylfluoride at a final concentration of 1 μmol L^{-1}, Gundersen et al. 1996) and were kept frozen until analysis (at −20°C in the field and −80°C once back in the laboratory). The bacteria were stained with 4′,6-diamidino-2-phenylindole (5 μg L^{-1} final concentration) and counted using epifluorescence microscopy (Zeiss Axiovert). Water samples were additionally collected onto glass fiber filters for the determination of chlorophyll *a* (Chl *a*) concentrations in surface waters. Filters were kept frozen at −80°C until pigments were extracted into 95% MeOH. Chl *a* was determined by high-pressure liquid

Fig. 1. Location of the two sampling sites as indicated by the stars.

chromatography using the method of Zapata et al. (2000), as adapted by Bonilla et al. (2005).

CO_2, CH_4, and O_2 concentrations—Dissolved CO_2 and CH_4 ($Gas_{(aq)}$) were determined by the equilibration of 2 liters of pond water into 20 mL of ambient air for 3 min, with the headspace sampled in duplicated vials (red stopper Vacutainer®) previously flushed with helium and vacuumed (Hesslein et al. 1990). Gas samples were taken within 5 min after collecting the pond water, and the ponds were sampled between 09:00 h and 18:00 h. Gas samples were kept at 4°C until analyzed by gas chromatography (Varian 3800 with a COMBI PAL head space injection system and a CP-Poraplot Q 25 m × 0.53 mm column and flame ionization detector). The dissolved gases were calculated according to Henry's Law:

$$\mathrm{Gas}_{(aq)} = K_H \times \mathrm{pGas} \quad (1)$$

where K_H is the Henry's constant adjusted for ambient water temperature, and pGas (pCO_2 or pCH_4) is the partial pressure of the gas in the headspace. Although the CO_2 equilibrium in pond water is linked to pH, the method used (equilibrium of a headspace a hundred times smaller than the water volume) was unlikely to change the pH sufficiently to affect dissolved CO_2 estimations. For CH_4, even though the effect was minor (< 1%), gas movement during the equilibration was corrected for.

Concentrations of CO_2, CH_4, and O_2 were followed in surface water (~ 20-cm depth) of one pond (KWK2; max depth of 2.6 m) during 8 d, from 28 June to 06 July 2007, using a continuous gas monitoring system. The monitor was first developed by the Canadian Department of Fisheries and Oceans and modeled after the design of Carignan (1998) and built by Environnement Illimité. Three types of sensors were used to measure CO_2 (infrared gas analyzer LI820, LI-COR), CH_4 (measurements in humid air; metal oxide sensor PN-SM-GMT, Panterra, Neodym Technologies), and O_2 (Qubit Systems) on a gas stream that was equilibrated with the source water. Details are given in Bastien et al. (2008). Briefly, water was pumped from the source via a reversible peristaltic pump through a bundle of porous polypropylene tubes (contactor, 1.0 × 5.5 Liqui-Cell Minimodule polysulfone, Membrana) that act as

Table 1. Limnological properties of the subarctic and arctic thaw ponds and lakes sampled in July 2007, including pH, total suspended solids (TSS), dissolved organic carbon (DOC), absorption coefficient by chromophoric dissolved organic matter at 320 nm (a_{320}), total phosphorus (TP), chlorophyll *a* (Chl *a*), bacterial abundance, and departure from gas saturation ($depCO_2$ and $depCH_4$) obtained from the difference between surface water concentration and the concentration in equilibrium with the atmosphere. RUN = pond formed in runnels over melting ice wedges; POL = pond on low-center polygons; KL = kettle lake; OL = oligotrophic lake; na = not available.

Pond name	Color or type	pH	TSS (mg L^{-1})	DOC (mg L^{-1})	a_{320} (m^{-1})	TP ($\mu g\ L^{-1}$)	Chl *a* ($\mu g\ L^{-1}$)	Bacteria ($\times 10^6$ cell L^{-1})	$depCO_2$* ($\mu mol\ L^{-1}$)	$depCH_4$* ($\mu mol\ L^{-1}$)
Whapmagoostui-Kuujjuarapik, Nunavik										
KWK1	brown	7.36	11.7	7.6	39.46	48.2	10.3	6.79	10.9	0.04
KWK2	black	8.46	5.1	5.2	30.99	37.6	2.4	9.86	23.2	0.04
KWK3	beige	6.97	42.0	8.7	41.85	52.8	6.4	12.79	47.6	0.29
KWK6	green	6.89	6.9	3.1	9.91	33.6	2.1	12.93	15.4	0.04
KWK7	brown	7.20	11.3	9.5	45.39	59.7	1.4	15.13	39.3	0.06
KWK11	black	6.77	9.5	9.4	38.29	95.6	23.8	15.23	10.3	0.05
KWK16	beige	6.53	24.3†	7.5	35.7†	na	5.2†	na	22.8†	0.44†
KWK21	beige	6.87	24.0	7.7	40.97	86.0	4.0	16.32	20.2	0.04
KWK23	beige	7.18	16.8	6.6	33.80	69.5	5.2	15.83	24.1	0.05
KWK33	brown	6.20	25.1	9.8	56.14	108.9	7.2	16.49	56.1	0.13
KWK35	brown	7.25	10.6	10.5	42.35	41.2	8.1	9.53	25.8	0.05
KWK36	black	6.52	8.0	8.1	40.38	36.9	2.1	10.34	45.8	0.11
KWK38	brown	7.33	5.5	6.0	19.50	54.2	1.9	10.52	38.8	0.43
Bylot Island, Nunavut										
BYL1	POL	9.6	3.3	10.4	13.48	26.6	0.8	13.84	−17.7	0.39
BYL22	POL	9.49	4.4	8.9	15.32	34.2	7.9	17.78	−17.1	0.17
BYL23	RUN	8.87	2.6	18.4	40.09	41.8	1.0	5.68	6.4	1.86
BYL24	RUN	8.99	6.2	11.0	24.21	43.0	3.8	6.70	−18.0	0.74
BYL25	RUN	8.08	4.0	12.4	23.76	16.7	0.5	10.93	36.9	0.63
BYL26	POL	9.59	2.8	10.8	13.17	18.0	1.0	7.91	−17.1	0.21
BYL27	RUN	8.54	4.5	14.4	45.99	28.6	1.5	14.68	78.1	5.17
BYL28	RUN	7.88	4.4	12.4	30.60	30.2	0.8	13.72	81.9	2.71
BYL29	POL	9.65	1.7	12.7	20.38	28.0	0.6	10.25	−16.5	0.19
BYL30	POL	9.46	5.7	10.7	13.40	26.5	7.4	10.25	−17.1	0.45
BYL31	POL	9.20	9.0	14.2	22.56	28.3	3.6	9.34	−16.5	0.94
BYL32	POL	9.61	5.0	10.4	15.56	26.2	7.3	17.73	−14.4	1.24
BYL33	RUN	9.38	1.5	8.2	14.86	14.3	1.0	4.67	−14.9	1.87
BYL34	POL	9.53	13.7	11.8	15.66	35.1	5.0	12.71	−16.5	0.35
BYL35	POL	9.40	3.3	8.7	14.36	35.4	1.9	9.95	−17.1	0.70
BYL36	POL	8.52	1.1	4.3	5.92	21.9	1.2	8.14	−10.8	0.05
BYL38	RUN	na	na	20.8	na	na	na	na		
BYL41	POL	7.19	na	8.9	13.20	20.8	2.9	8.38	−18.7	0.16
BYL42	POL	8.11	na	11.3	15.88	4.2	1.5	2.23	−14.5	0.12
BYL37‡	KL	8.13	1.8	5.2	18.43	16.5	1.8	7.37	−7.5	0.02
BYL39‡	OL	7.06	1.4	1.5	4.70	3.2	0.9	1.61	−2.7	0.02
BYL40‡	OL	7.18	na	1.5	3.79	3.6	0.6	1.20	0.6	0.04

* Average gas concentrations in equilibrium with the atmosphere for the 2007 data series are as follows (if concentrations are preferred to departure from saturation): 19.5 $\mu mol\ L^{-1}$ CO_2 and 0.0034 $\mu mol\ L^{-1}$ CH_4.
† Values not available in 2007 but results from 2006 are given as an indication.
‡ Three lakes are shown for comparison.

a water–air exchanger. Solenoid valves controlled the gas flow from the contactor to the air as required. Water and air temperatures were also recorded. Control of all electrical devices and collection and storage of data were performed by an electronic data logger (CR10X, Campbell Scientific). The entering water was filtered using layers of Nitex of 250, 100, 53, and 10 μm. Measurements were taken automatically every 3 h (the monitoring operating cycle took 22 min: one cycle of 20 min in water with two measurements at 10 and 20 min, and one cycle of 2 min in air with one measurement). Duplicate measures taken by the system had on average a standard deviation of 1.8 $\mu mol\ L^{-1}$. Variations in water flow rate through the contactor were caused by Nitex clogging at the end of $\sim$ 2 d (from 600 down to 150 mL min^{-1}), but in most cases the filters were changed daily to reduce this effect.

Estimation of fluxes with floating chamber and gas partial pressure—In 2007, CO_2 flux was directly estimated using a floating chamber (area = 0.179 m^2; volume =

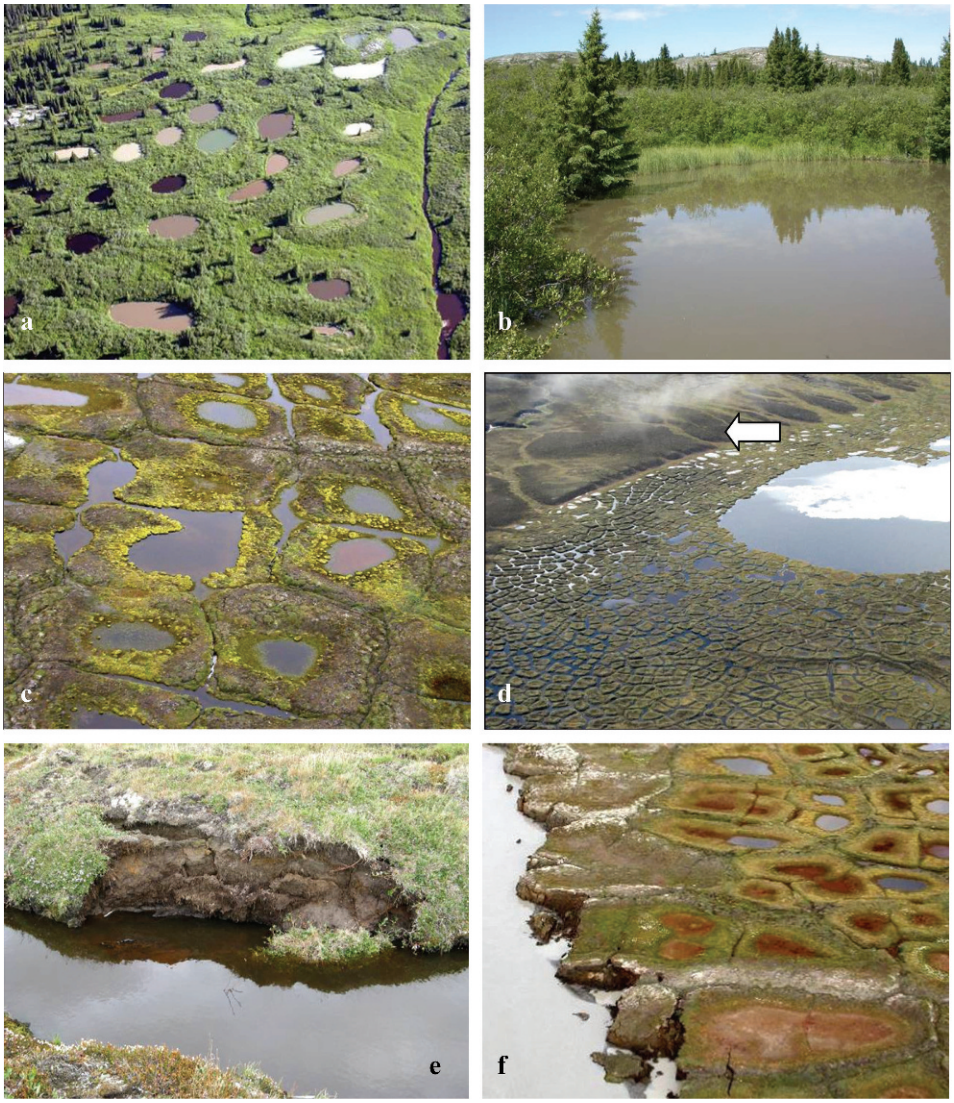

Fig. 2. Thaw pond study sites. (a) Subarctic thaw ponds (12–30-m diameter), (b) dense shrubs around a turbid subarctic pond, (c) thaw ponds on low-center polygons (~10–20-m diameter) and in runnels (~1–4-m wide) over melting ice wedges in the arctic site, (d) general view of the arctic site on the side of a moraine (arrow) with a larger pond similar to BYL36 (white color is floating ice), (e) soil erosion beside an arctic thaw pond (~1-m wide), (f) orange benthic mat exposed to the air after a long period without rain in 2007, and peat layer erosion along the bank of the proglacial river.

0.0175 m^3) connected to an infrared CO_2 analyzer (EGM-4, PP-Systems) in a closed path, and the equation:

$$\text{Flux} = (S \times \text{MW} \times V_{\text{ch}})/(V_{\text{m}} \times A_{\text{ch}}) \times F \quad (2)$$

where S is the slope from the graph of gas concentration in the chamber vs. time (measurements taken for 25 to 60 min depending on flux rate), MW is the gas molecular weight, V_{ch} is the volume of the chamber, V_{m} is the molar volume of the gas at ambient temperature, A_{ch} is the area of the chamber, and F is a unit conversion factor to obtain a flux value in mg gas m^{-2} d^{-1}.

CO_2 and CH_4 fluxes were also estimated for all the ponds studied in 2007 using dissolved gas concentrations, wind speed, and a wind-based equation for the gas transfer:

$$\text{Flux} = \text{k}\left(C_{\text{sur}} - C_{\text{eq}}\right) \quad (3)$$

where k is the gas transfer coefficient (cm h^{-1}), C_{sur} is the gas concentration in surface water (μmol L^{-1}), and C_{eq} is the gas concentration in equilibrium with the atmosphere (for the time series, direct measurements of gas concentration in the air were used instead of global atmospheric values as for all the other ponds). The gas transfer coefficient for a given gas was calculated as:

$$\text{k} = \text{k}_{600}(\text{Sc}/600)^{-0.5} \quad (4)$$

Table 2. Comparison of 12 subarctic ponds sampled both in 2006 and 2007 and of 18 arctic ponds (sampled in 2007). Surface water temperature at sampling (T), dissolved organic carbon (DOC), DOC-specific absorption coefficient at 320 nm (a_{320}:DOC), and departure from gas saturation ($depO_2$, $depCO_2$, and $depCH_4$) obtained from the difference between surface water concentration and the concentration in equilibrium with the atmosphere. Range shown is minimum–maximum. Average ± SD in parentheses.

Parameter	Sampling period		
	KWK 21–27 July 2006	KWK 28 June–04 July 2007	BYL 15–23 July 2007
T (°C)	16.4–22.7(19.7±1.7)	9.5–19.5(13.4±3.4)	7.0–12.0(10.4±1.6)
DOC (mg C L^{-1})	3.8–12.9(8.8±2.7)	3.1–10.5(7.7±2.1)	4.3–18.4(11.1±3.0)
a_{320}:DOC (L mg C^{-1} m^{-1})	2.2–4.8(3.9±0.7)	3.2–6.0(4.7±0.9)	1.2–3.2(1.7±0.5)
$depO_2$ (μmol L^{-1})	−60–17(−12±28)	−32–47(−3±21)	−87–59(17±43)
$depCO_2$ (μmol L^{-1})	4–79(42±20)	10–56(30±15)	−19–82(−1±32)
$depCH_4$ (μmol L^{-1})	0.23–1.34(0.48±0.33)	0.04–0.43(0.11±0.12)	0.05–5.2(1.0±1.3)

$$k_{600} = 2.07 + 0.215 \times U_{10}^{1.7} \quad (5)$$

where the value k_{600} is the gas exchange coefficient given by Cole and Caraco (1998) that is dependent on wind speed at 10-m height (U_{10}), and Sc is the Schmidt number of that gas calculated from empirical third-order polynomial fits to water temperature and corrected for Sc at 20°C (600). Wind speed was averaged over the preceding hour.

We computed gas fluxes using the three hourly data from the continuous gas monitoring system using three different models for gas exchange. We used two wind-based models for the gas transfer coefficient, that of Cole and Caraco (1998) described above and one we derived using estimates of k_{600} based on eddy covariance measurements in an oligotrophic subarctic lake (Jonsson et al. 2008). With nonnegative values of k the regression is:

$$k_{600} = 0.81 + 1.087U_{10} + 0.085U_{10}^2 \quad (6)$$

We also used the small eddy version of the surface renewal model (MacIntyre et al. 1995), which takes into account physical processes in addition to wind that cause turbulence at the air–water interface (Banerjee and MacIntyre 2004). For this method, we calculated surface energy fluxes from the meteorological data and surface water temperatures measured with the continuous gas monitoring system following MacIntyre et al. (2002). We then computed the turbulence in the upper mixed layer following Imberger (1985) and MacIntyre et al. (1995). Since we only had surface water temperatures, we ran the computation for mixed layer depths of 0.1, 0.3, and 1 m, since profile data from KWK2 and the nearby ponds indicated mixed layers that were typically 0.1–0.3 m in depth during the day. Near uniform profiles of O_2 and CO_2 to 1 m indicated that nocturnal mixing might penetrate as deep as 1 m. We assumed net longwave radiation was −50 W m^{-2}, a value typical for somewhat cloudy days in the northern temperate zone and the Arctic (MacIntyre et al. 2009). Values of the gas transfer coefficient for all models were averaged over 3 h and then used to calculate fluxes.

Results

Pond limnological characteristics—Overall, the thaw ponds in subarctic and arctic regions were biologically productive ecosystems, with an average bacterial abundance of 11.2 × 10^6 cells mL^{-1} (measured in 2007 only), Chl *a* concentrations of 4.9 μg L^{-1}, and total phosphorus concentration of 51 μg L^{-1} (Table 1 shows the 2007 data series; *see* Table 2 for comparison of ranges between both years). The pH varied from 5.8 to 9.7, with the arctic ponds showing the highest pH values. The subarctic ponds presented striking patterns of colors (Fig. 2a) generated by differing combinations of suspended particles (mostly clays and silts; total suspended solids [TSS] averaged 20.0 mg L^{-1}), dissolved organic matter content, and CDOM absorption properties (DOC averaged 8.3 mg L^{-1}; absorption coefficient at 320 nm [a_{320}] averaged 35.0 m^{-1}). The arctic ponds had lower TSS (average of 4.6 mg L^{-1}), higher DOC (11.6 mg L^{-1}), but lower CDOM (a_{320} average of 19.9 m^{-1}), and less productive pelagic waters (average of 2.8 μg Chl *a* L^{-1} and 27 μg [TP] L^{-1}) compared to the subarctic ponds. However, thick microbial mats were observed in ponds formed on low-center polygons, with a consortium of taxa dominated by oscillatorian cyanobacteria (Vézina and Vincent 1997). The mats were actively photosynthesizing under the continuous light exposure of the polar summer and most likely the cause of higher pH values and low nutrients in the water column.

Different conditions were observed at the arctic sites in the 2 yr, likely generated by variations in hydrology and climate. The snow pack was relatively thin at the end of winter in 2007 (21 cm on 01 June compared to a long-term average of 31 cm; G. Gauthier unpubl. data); temperatures were exceptionally warm, and relative humidity low in 2007 (10 mm of rain in July). Therefore, several of the ponds sampled in 2006 had completely dried up in 2007, and in some cases retained their orange benthic microbial mats that became exposed to the air (Fig. 2f).

Dissolved gases in surface waters—All subarctic ponds were supersaturated in both CO_2 and CH_4. Similarly, all arctic ponds were supersaturated in CH_4; however, they were mostly undersaturated in CO_2 (Table 1). Global values of atmospheric partial pressures (IPCC 2007; 38.4 Pa of CO_2 and 0.18 Pa of CH_4) were used to determine the gas saturation (when converted to aqueous concentrations at equilibrium using ambient water temperatures, these values corresponded on average to 19.5 μmol L^{-1} of CO_2 and 0.0034 μmol L^{-1} of CH_4). At the subarctic site,

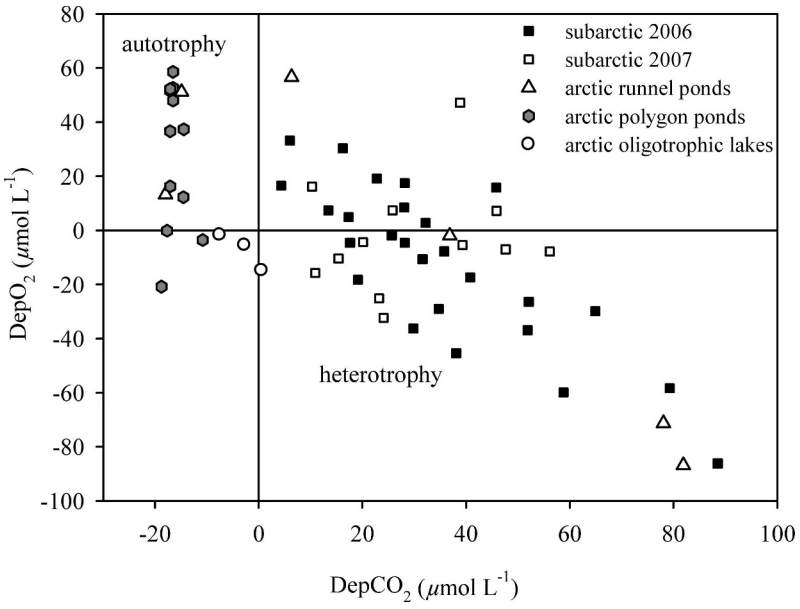

Fig. 3. Correlation between O_2 and CO_2 (departure from gas saturation, $depO_2$ and $depCO_2$) in subarctic thaw ponds (squares), arctic thaw ponds (polygon ponds, polygons; runnel ponds, triangles), and arctic lakes (circles).

differences in dissolved gases (departure from saturation is used to account for temperature differences among ponds and years) were observed between 2006 and 2007 (using the 12 ponds that were sampled in both years), with lower CO_2 (paired t-test, $t = 2.051$, df = 11, $p = 0.065$) and substantially lower CH_4 concentrations in 2007 ($t = 4.932$, df = 11, $p < 0.001$; Table 2). Departure from CO_2 saturation was inversely correlated with departure from O_2 saturation (Fig. 3; $r = -0.733$, $p < 0.0001$, $n = 59$) and positively correlated with DOM chromophoric properties such as a_{320} ($r = 0.619$, $p < 0.0001$, $n = 63$) or DOC-specific a_{320} ($r = 0.584$, $p < 0.0001$), but not with DOC ($r = 0.107$, $p = 0.402$). The correlation with DOC improved when subarctic data were tested alone ($r = 0.431$, $p = 0.004$).

Profiles of temperature and gas concentrations—Despite their shallowness (maximum measured depth varied from 0.8 to 3.3 m), most of the subarctic ponds were thermally stratified at the times of sampling (Fig. 4). KWK36 was stratified to the surface (no mixed layer), while the others had mixed layer depths of ~ 0.1 to 1 m. The stratification resulted from the high attenuation of light in these systems due to high concentrations of DOC and suspended solids. The Brünt Väisälä frequency (N) was calculated as an index of water column stability $N = (g/\rho_{max} \times \Delta\rho/\Delta z)^{1/2}$, where g is the acceleration due to gravity (9.8 m s^{-2}), ρ_{max} is the maximum density of the considered water column, and $\Delta\rho/\Delta z$ is the vertical density gradient. N varied from 0.04 to 0.10 s^{-1} in the subarctic ponds (average 0.06 s^{-1}; $n = 13$; maximum depth of 3.3 m) and from 0.01 to 0.09 s^{-1} in those arctic ponds that were deep enough to obtain a profile (average 0.05 s^{-1}; $n = 5$; maximum depth of 1 m). The arctic lakes (maximum depths of BYL37, BYL39, and BYL40 were 3.2, 4.3, and 6.7 m, respectively) had a stability index lower than 0.023 s^{-1}.

Most subarctic ponds also had a hypoxic hypolimnion, with on average 23% of surface oxygen at the bottom of the hypolimnion (1.4% to 95%; $n = 13$). In most cases (11 out of 12 ponds profiled), dissolved CO_2 and CH_4 increased in the bottom waters, with on average 10 times more CO_2 (up to 24×) and 744 times more CH_4 (up to 2802×) at the bottom of stratified ponds, 10–20 cm above sediments. Surface CO_2 concentrations were not correlated with bottom values, but CO_2 and CH_4 concentrations above the sediments were significantly correlated ($r = 0.886$, $p < 0.0001$). The rapid increases in CO_2 and CH_4 and decrease in O_2 at ~ 1-m depth in these ponds indicates that this is a typical depth of nocturnal mixing and that mixing events to slightly deeper depths will entrain significant quantities of GHG to the surface. Gas profiles were not performed in the arctic ponds because of their shallowness.

Time series temperatures in pond KWK16—The yearlong monitoring of surface and bottom water temperatures of subarctic pond KWK16 revealed persistent stratification despite its shallow depth (Fig. 5). The temperature difference between surface and bottom waters was larger than 1°C for 87% of the year, with summer stratification occurring about 34% of the year (increasing to 42% with a stability criterion of 0.5°C difference between surface and bottom temperatures). Temperature inversions occurred on 28 October and 17 May. Winter water temperatures ranged between 2°C and 4°C and indicated that the pond did not freeze. The ice was likely thin and covered by a thick layer of snow (total snowfall in 2007 at the village of Whapmagoostui-Kuujjuarapik was 2.4 m, but the snow likely accumulates on ponds due to the local topography), since the temperature at 0.15-m depth always remained above 0.08°C (winter average of 0.7°C). There were two principal periods of mixing: one long episode beginning in

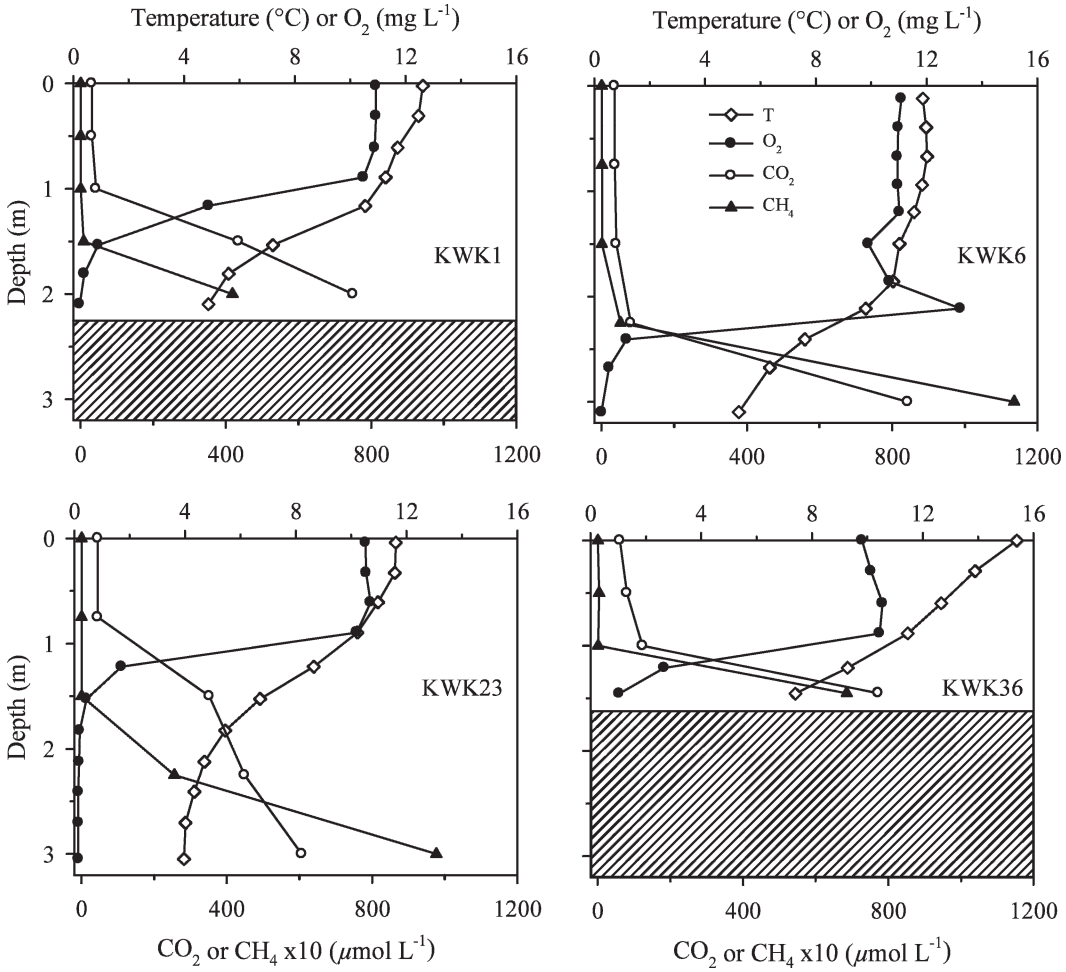

Fig. 4. Profiles of temperature and dissolved concentrations of O_2, CO_2, and CH_4 in four subarctic ponds (CH_4 were multiplied by 10 to fit CO_2 scale).

September until the end of October (but during which diurnal stratification was still occurring; Fig. 5b) and a short episode in May (Fig. 5c). Isolated mixing events of the whole water column were also observed during the summer (defined here as 01 June to 03 September), but on only two occasions in July, while the temperature difference between surface and bottom waters still remained above 0.2°C. However, the analysis of heat fluxes in one pond (KWK2, less turbid) revealed regular mixing events in the upper water column (*see* below).

Meteorological and gas measurements time series from pond KWK2—As in the other subarctic ponds, shallow mixed layers were observed in pond KWK2. During the study period, air temperatures were lower than surface water temperatures except on the two sunniest days, 02–03 July (Fig. 6). Relative humidity, typically above 80%, decreased on sunny days. Effective heat flux, which indicates whether the uppermost mixing layer will gain or lose heat, was well above 0 W m^{-2} on sunny days, indicating that the upper water column would have stratified on those days (Fig. 7). Cold, cloudy, windy conditions prevailed during the last 2 d of the study. Evaporation caused the greatest heat loss and increased during windy periods (Fig. 7a). The effective heat flux was always negative at night as well as throughout most of the cloudy days (Fig. 7b) and would cause mixed layer deepening at those times.

Oxygen concentrations were in near equilibrium with the atmosphere except on the afternoons of 02–03 July (Fig. 7c). The increased concentrations likely indicated increased photosynthesis due to higher insolation (significant correlation obtained between the departure to O_2 saturation and incident irradiance, $r = 0.393$, $p = 0.0017$) and reduced exchanges with the atmosphere due to suppressed mixing on those days. From 04 to 06 July, concentrations were below saturation. CO_2 concentrations always exceeded saturation, indicating the pond was net heterotrophic (dissolved CO_2 varied from 26.7 to 81.9 μmol L^{-1}, with an average of 51.1 μmol L^{-1}). Methane concentrations began to increase substantially relative to saturation on 02 July. Fluctuations in concentrations (or departure from saturation) in these three gases tended to coincide (positive correlation between CO_2 and CH_4 and

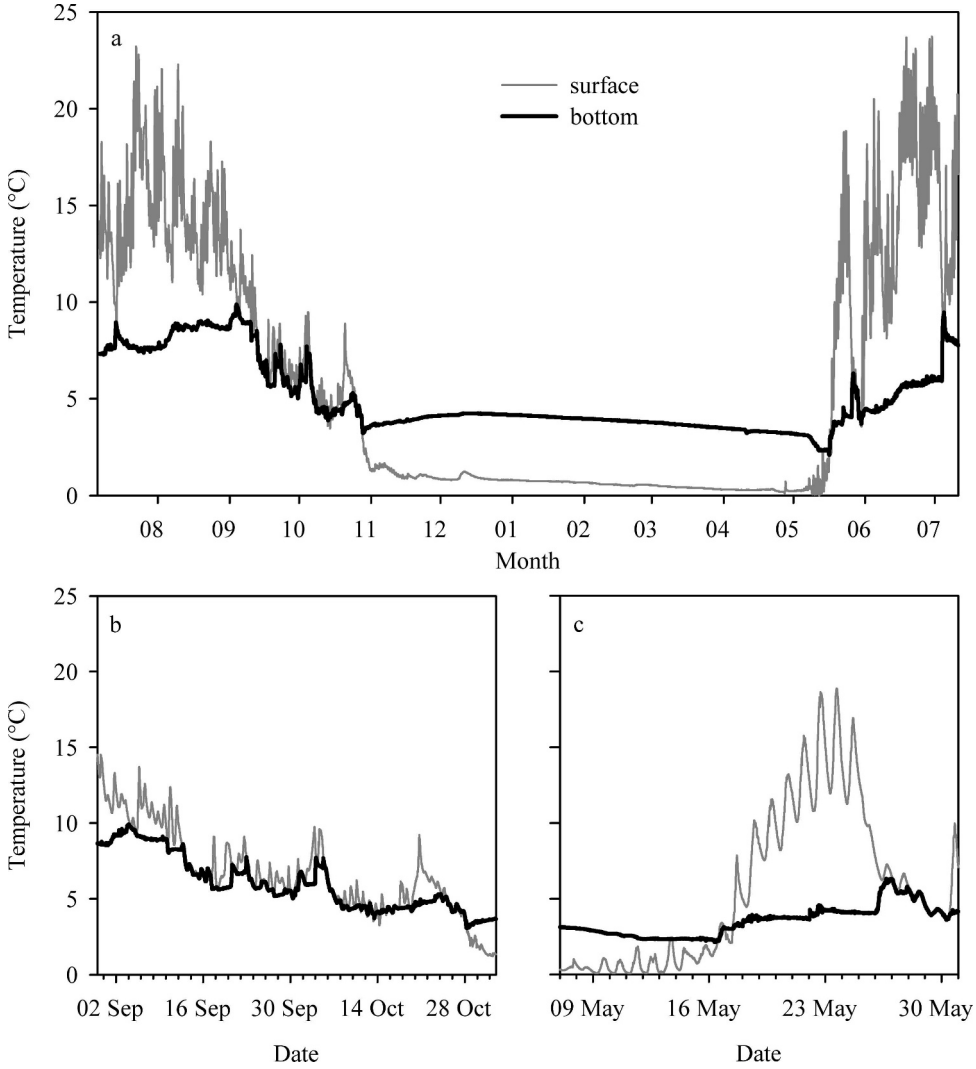

Fig. 5. Temperature at the surface (0.15 m) and bottom (2.0 m) of pond KWK16 (maximal depth ~2.2 m) (a) followed over one complete year from 06 July 2007 to 11 July 2008, (b) showing diurnal stratification during the autumnal mixing period, and (c) during spring mixing.

negative correlation between CO_2 and O_2; $r > \pm 0.639$, $p < 0.0001$). The largest increases in CO_2 and largest decreases in O_2 occurred at the end of the day on 03 July. CH_4 concentrations also increased along with CO_2. These changes co-occurred with the effective heat flux decreasing below zero, which signifies mixed layer deepening. Similar patterns were observed the preceding day (02 July). The lower O_2 concentrations on 04 and 05 July were likely due to lower photosynthesis (lower irradiance on cloudy days), but the concomitant sustained higher concentrations of CO_2 and CH_4 also indicate a deepening of the mixed layer and the associated entrainment of dissolved gases from deeper waters. Profile data taken on 07 July indicated that gas concentrations were uniform to at least 0.75 m, which supports the idea that mixing occurred during the cold front at the end of the study period.

The gas transfer coefficients k computed using the data in Jonsson et al. (2008) were on average 40% higher than those computed following Cole and Caraco (1998) and up to 60% higher at the highest wind speed (Fig. 8). Higher k values based on the eddy covariance data are not surprising since eddy covariance provides fluxes on the timescale of the meteorological forcing (e.g., minutes to hours). Since GHG fluxes increase nonlinearly with wind speed, k estimates based on fluxes computed over timescales of days will be underestimates. Estimates of k with the surface renewal model depended upon the assumed mixed layer depth, with higher estimates for shallower mixed layers as the flux of energy, which induces mixing, is then trapped in a smaller volume of water. Estimates of k using surface renewal were similar to those from Cole and Caraco (1998) assuming the upper mixed layer was 1-m deep and similar to those obtained from eddy covariance data assuming a mixed layer of 0.1 m. As anticipated, the surface renewal model often gave higher values at night as it captured the effects of turbulence from heat loss. Because k estimated from surface renewal was bounded by the two other approaches and because we did not have time series

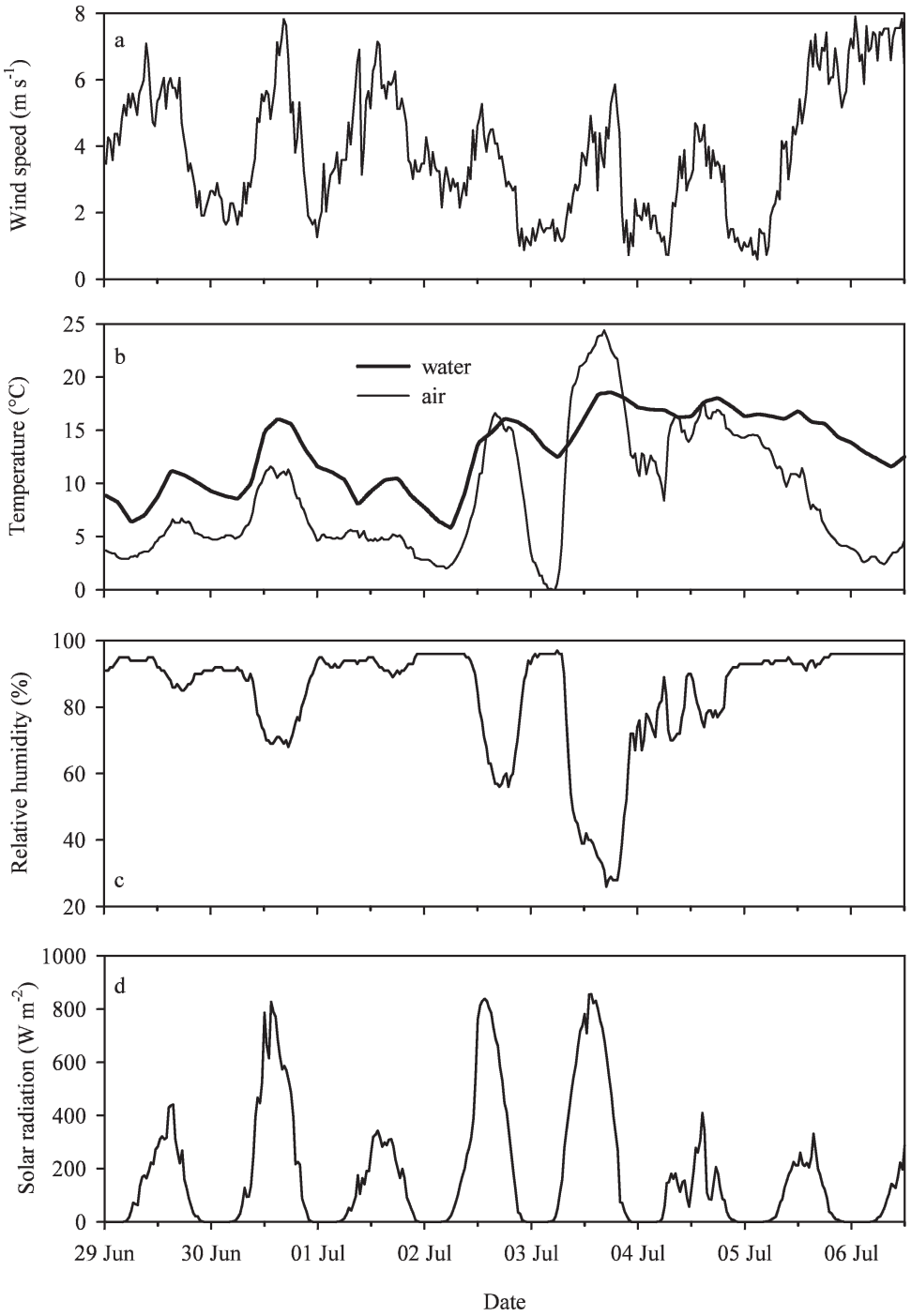

Fig. 6. (a) Wind speed at 10-m aboveground, (b) air (thin line) and water (thick line) temperatures, (c) relative humidity, and (d) incident shortwave radiation (300–1100 nm) at pond KWK2 during the 8-d period of gas measurements in surface water.

measurements of mixed layer depth, we do not present fluxes computed with this method. The highest GHG fluxes occurred on 30 June and on 05 and 06 July (Fig. 9) in response to the higher wind speed on those days (Fig. 6). Sustained high fluxes at the end of the study were additionally caused by the increased gas concentrations in the upper water column due to the increased vertical mixing induced by cooling.

Gas fluxes in pond data series—Gas fluxes varied widely in thaw ponds data series (by 242% for CO_2 and by 195% for CH_4). The lowest CO_2 fluxes were obtained in arctic polygon ponds (down to -20.5 mmol m^{-2} d^{-1}), and the highest CO_2 and CH_4 fluxes were obtained in arctic runnel ponds (up to 114.4 and 5.6 mmol m^{-2} d^{-1} of CO_2 and CH_4, respectively). The method used to measure CH_4 concentration in water (2 liters of pond water in equilibrium with 20-mL headspace)

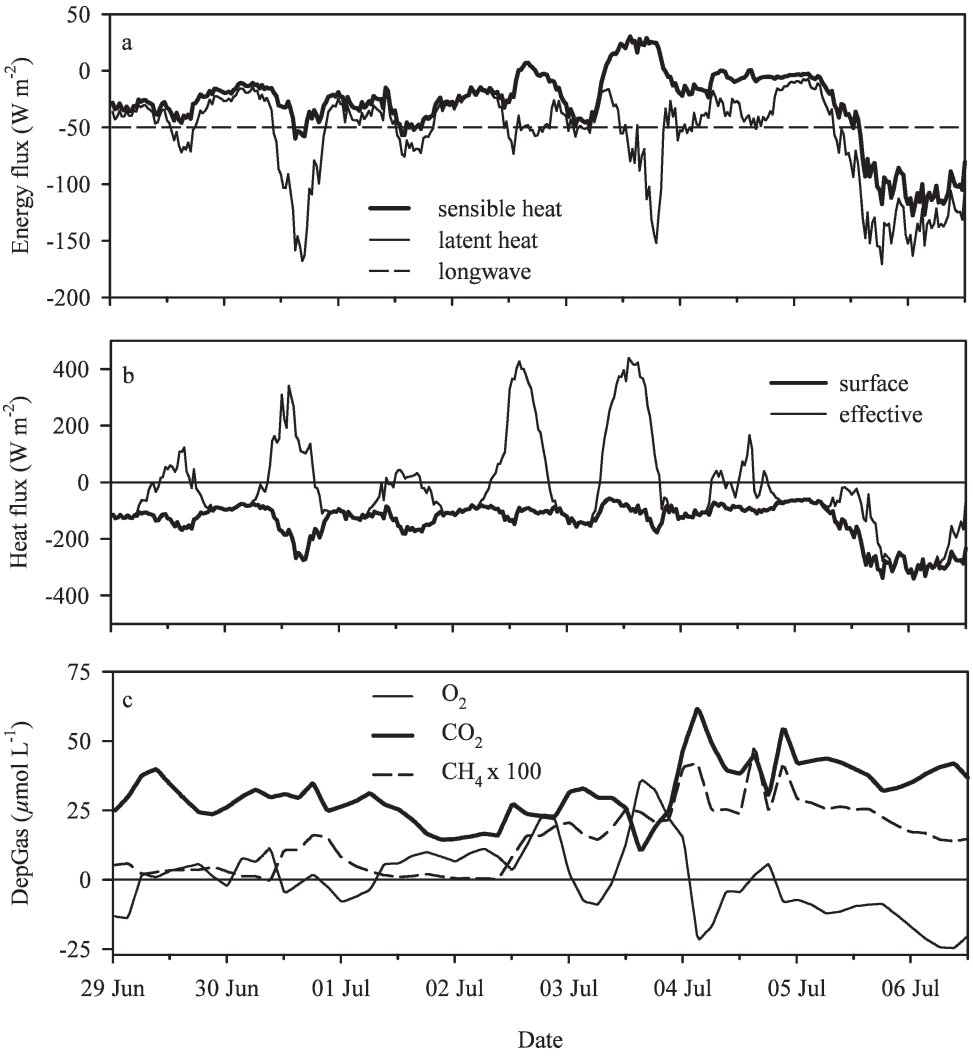

Fig. 7. (a) Sensible heat (thick line), latent heat (thin line), and longwave (dashed line) fluxes, (b) surface heat flux (sum of sensible, latent, and net longwave, thick line) and effective heat flux (sum of net shortwave and surface heat flux, thin line), and (c) difference between concentration of O_2 (thin), CO_2 (thick), and CH_4 (dashed) in surface water and the gas concentration in equilibrium with the atmosphere (depGas) of pond KWK2. Difference for CH_4 has been multiplied by 100. Effective heat flux was computed assuming that the mixing layer was 0.3-m deep.

for estimation of fluxes with the wind-based model most likely excluded CH_4 bubbles (especially those from sporadic bubbling on thaw lake edges as described in Walter et al. 2006). Therefore, these values must be considered diffusive fluxes (although the influence of small bubbles cannot be excluded; Semiletov et al. 1996) that provide a lower bound to total CH_4 flux. Also, wind speed varied from 0.2 to 8.4 m s^{-1} in July, generating variability in gas fluxes possibly of the same order of magnitude as spatial variations. For example, this range in wind speeds would generate CH_4 fluxes from 0.4 to 1.8 mmol m^{-2} d^{-1} in pond BYL31. Therefore, the values presented here, obtained from one discrete measurement during the day, should be considered first approximations.

The CO_2 fluxes obtained directly with the floating chamber in 2007 (Table 3) were correlated with those from the same ponds estimated from dissolved gas concentration following Cole and Caraco (1998; for paired fluxes, $r = 0.842$, $p < 0.0001$, $n = 27$). However, fluxes obtained with the floating chamber were generally lower than with the wind-based model (mean of 4 compared to 12 mmol m^{-2} d^{-1}, respectively), although those measurements were not always taken exactly at the same time as the dissolved gases.

Discussion

The two groups of thaw pond systems in this study showed striking differences in their morphological, physicochemical, and biological properties, and they also contrasted in their greenhouse gas characteristics. Even at the local scale, there was large variability between nearby waters. We measured negative CO_2 fluxes (net transfer from atmosphere to water) in arctic ponds colonized by

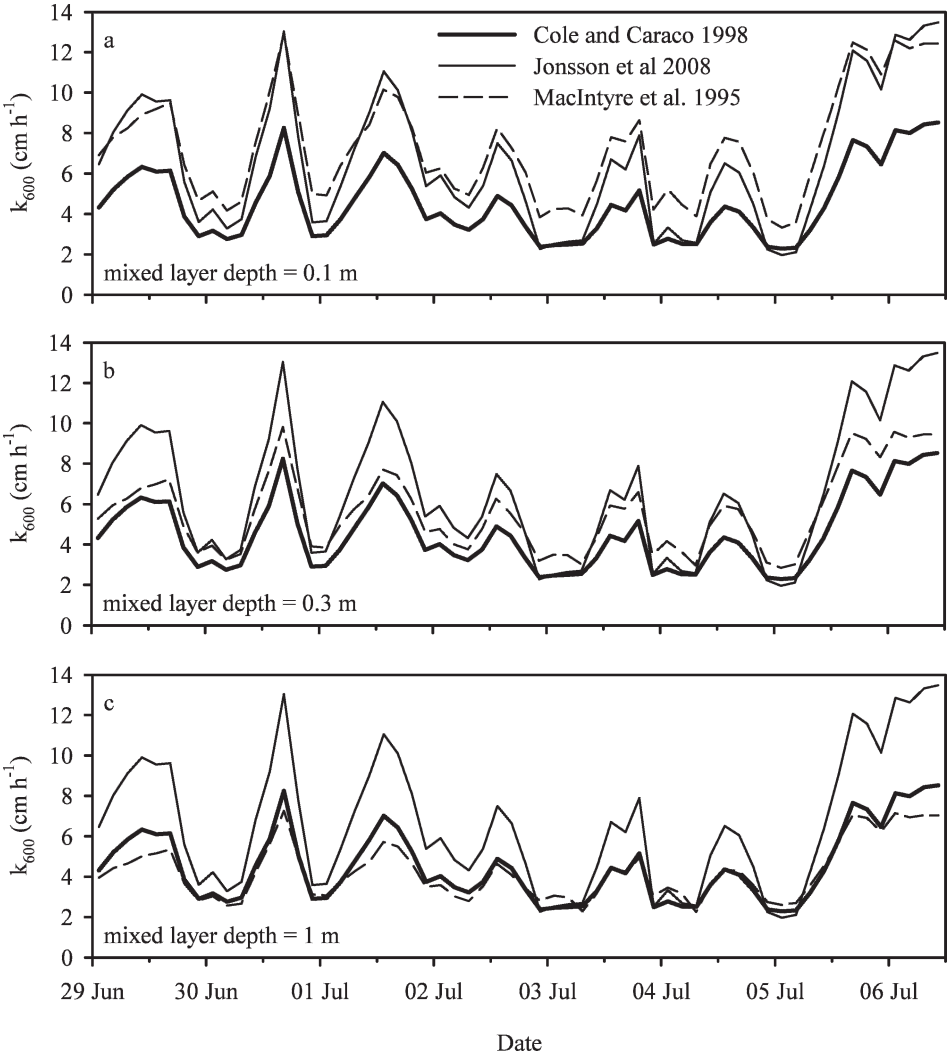

Fig. 8. Gas transfer coefficients calculated following Cole and Caraco (1998; thick line), Jonsson et al. (2008; thin line), and the surface renewal model (MacIntyre et al. 1995; dashed line) with surface renewal calculations assuming a mixed layer depth of (a) 0.1 m, (b) 0.3 m, and (c) 1 m.

benthic microbial mats, while the largest positive fluxes occurred in the adjacent humic-rich runnel systems. Gas exchange also varied greatly over all measured timescales: diel, weekly, and seasonal.

Supersaturated thaw ponds—Like most lakes and ponds of the temperate and boreal regions, the Canadian subarctic thaw ponds sampled in the present study were all supersaturated in CO_2, with concentrations varying from 20 to 105 μmol L^{-1}, corresponding to a partial pressure range of 44 to 230 Pa (n = 43, data from 2006 and 2007 combined). These values fall in the range obtained further to the south in a large survey of boreal lakes showing surface water CO_2 partial pressure between $\sim$ 40 and 250 Pa (n = 2838; Sobek et al. 2005). Subarctic thaw ponds were also supersaturated in CH_4 (concentration varying from 0.04 to 1.34 μmol L^{-1}, or 0.1 to 3.1 Pa), with large increases observed in the isolated hypolimnion (*see* below). The automated measurements in pond KWK2 over 8 d (Fig. 7) give a sense of the short-term dynamics in CO_2 (ranging from 27 to 82 μmol L^{-1}) and CH_4 (from 0.02 to 0.56 μmol L^{-1}) that can occur in surface waters of a thaw pond in summer. Dissolved CH_4 varied to a larger extent than CO_2 in this time series (coefficients of variation of 69% and 19%, respectively), consistent with the results of Walter et al. (2006).

It is instructive to compare the results from 2 yr sampled at different dates (end of July in 2006 and 3 weeks earlier in 2007; Table 2). Earlier in summer 2007, the surface water temperature was colder, dissolved O_2 concentration was higher, and both CO_2 and CH_4 were lower. While these data could be indicative of reduced heterotrophic activity, they could also reflect more efficient exchanges with the atmosphere (negative effective heat flux) and/or lower accumulations of gases in deeper waters. Nevertheless, they indicate the high spatial and temporal resolution of

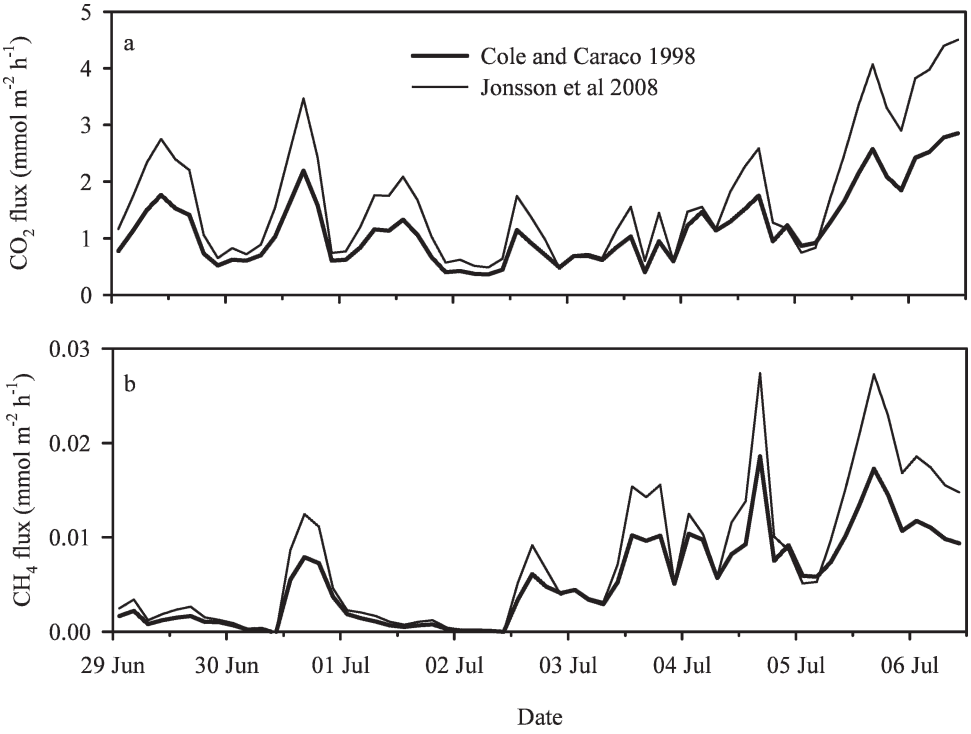

Fig. 9. Greenhouse gas fluxes computed using the two wind-based models for the gas transfer coefficient: Cole and Caraco (1998; thick line) and Jonsson et al. (2008; thin line). (a) CO_2, (b) CH_4.

meteorological data, water column structure, and gas concentrations that are required to fully define GHG dynamics.

The arctic waters differed in their GHG characteristics. These ponds were often undersaturated in CO_2, principally when benthic cyanobacteria had developed active photosynthetic mats (in low-center polygon ponds; although in 2008, several runnel ponds were colonized by *Sphagnum* spp. that likely also contributed to the CO_2 sink). However, the arctic ponds generally had higher CH_4 contents than the surface waters of subarctic ponds (Table 2). Other studies found the opposite trend, with larger CH_4 concentrations in sites located at lower latitudes (71.5°N compared to 68.5°N in Semiletov et al. 1996 and Nakano et al. 2000). The ponds developing on the periphery of polygons were in most cases supersaturated in both gases (average dissolved CO_2 and CH_4 were 48.8 and 2.2 μmol L^{-1} in runnel ponds, compared to 3.8 and 0.4 μmol L^{-1} in low-center polygon ponds, respectively), and the concentration differed significantly between the two pond types (Mann–Whitney rank sum test, $p < 0.008$). The runnel ponds had high DOM and especially high chromophoric DOM (on average $a_{320} = 30$ m^{-1} and DOC = 13 mg L^{-1}), whereas polygon ponds apparently had photobleached DOM (a_{320} : DOC 1.6 times lower than in runnel ponds, with on average $a_{320} = 15$ m^{-1} and DOC = 10 mg L^{-1}). Therefore, photolysis of DOM into CO_2 was possibly acting with greater importance in the shallow arctic ponds exposed to longer daylight as compared to the turbid subarctic ponds. In the kettle lake and especially the two oligotrophic lakes, dissolved CO_2 (on average 17 μmol L^{-1}) and CH_4 (on average 0.03 μmol L^{-1}) were close to atmospheric equilibrium. These lakes had the lowest bacterial abundance (especially the oligotrophic lakes) and DOM concentration. Therefore, reduced inputs of allochthonous organic carbon and nutrients in these lakes likely dampened their role as gas conduits to the atmosphere.

Several factors are known to influence dissolved CO_2 in freshwaters, including DOM concentrations, availability to microbes, reactivity to sunlight (Granéli et al. 1996; Obernosterer and Benner 2004), vertical structure of the water column, benthic-pelagic coupling, type of microbial assemblages (Huttunen et al. 2006; Kankaala et al. 2006), uptake by primary producers in productive ecosystems (del Giorgio et al. 1999), and inputs by groundwater and stream flow (Striegl and Michmerhuizen 1998). Groundwater and stream flow inputs were found to be minor in temperate and dystrophic bog lakes (Hanson et al. 2003) and are likely reduced in thaw ponds: their closed morphology and the presence of permafrost limit water circulation. This is particularly the case for the subarctic thermokarst ponds studied that are located in impermeable clay–silt beds (although small streamlets through breaches between adjacent ponds were sometimes observed). Therefore, the CO_2 supersaturation observed in surface waters of thaw ponds is thought to originate mainly from three sources: benthic respiration, pelagic respiration, and DOM photolysis. Jonsson et al. (2001) demonstrated that 40% of dissolved CO_2 originated from benthic respiration, 50% from pelagic respiration, and 10% from DOM photolysis in a deep humic lake in Sweden. A much larger contribution of benthic respiration is likely in shallow ponds (Kortelainen et

Table 3. Gas fluxes measured with the floating chamber (CO_2) compared to estimations from dissolved gas concentration and wind speed following Cole and Caraco (1998). na = not available.

Pond name	CO_2 flux chamber (mmol m^{-2} d^{-1})	CO_2 flux wind speed (mmol m^{-2} d^{-1})	CH_4 flux wind speed (mmol m^{-2} d^{-1})	O_2 flux wind speed (mmol m^{-2} d^{-1})
Whapmagoostui-Kuujjuarapik, Nunavik				
KWK1	2.3	8.9	0.04*	−13.6
KWK2	10.6	19.3	0.04*	−22.1
KWK3	na	30.1	0.18	−4.7
KWK6	5.2	18.3	0.05*	−13.0
KWK7	24.3	36.7	0.05	−5.4
KWK11	4.3	13.0	0.06	21.7
KWK16	10.3	na	na	na
KWK21	3.5	13.5	0.03*	−3.1
KWK23	23.2	35.0	0.07*	−49.4
KWK33	11.1	62.2	0.14	−9.2
KWK35	4.8	16.2	0.03	4.9
KWK36	na	39.2	0.09	6.6
KWK38	14.0	40.8	0.45	52.6
Bylot Island, Nunavut				
BYL1	−14.6	−14.3*	0.32	−0.1
BYL22	−10.8	−19.9*	0.20	20.0
BYL23	−3.1	8.0	2.33	75.3
BYL24	−2.3	−20.5*	0.84	16.0
BYL25	16.3	20.3	0.35	−1.2
BYL26	−14.9	−9.8*	0.12	31.4
BYL27	23.9	85.4	5.62	−82.3
BYL28	28.2	114.4	3.77	−127.2
BYL29	−18.2	−11.9*	0.14	40.0
BYL30	−17.1	−13.0*	0.34	29.5
BYL31†	−9.7	−11.8*	0.67	36.4
BYL32†	−11.1	−10.1	0.87	27.7
BYL33†	−7.0	−10.6	1.32	38.4
BYL34	−13.8	−8.0*	0.17	30.1
BYL35	−8.3	−12.6*	0.52	40.8
BYL36	−3.2	−6.6	0.03	−2.3
BYL38	60.0	na	na	na
BYL41	na	−8.9	0.08	−10.3
BYL42	31.5	−6.6	0.05	5.9
BYL37‡	−1.4	−5.3	0.01	−1.3
BYL39‡	3.5	−1.5	0.01	−3.3
BYL40‡	5.9	0.4	0.03	−11.6

* Dissolved CO_2 or CH_4 in surface waters were close to the detection limit. This detection limit was used to calculate the gas flux, thus, those values are only approximate.

† These ponds were localized in another valley on Bylot Island, at ca. 10 km north of the climate station; therefore, wind-based estimations in gas flux are given only as an indication.

‡ Three lakes are shown for comparison.

al. 2006). In the turbid subarctic thaw ponds where light is rapidly attenuated (reduced production of CO_2 by DOM photolysis), surface water CO_2 was most likely derived from the respiration in littoral sediments located above the metalimnion (Bastviken et al. 2008) and, following vertical mixing at night and during cold fronts, from respiration deeper in the water column and from the sediments.

Stratified thaw ponds—A major consequence of the high turbidity and humic content of subarctic thaw ponds, combined with the low evaporation, high solar radiation, and warm air temperatures typical near ice-off, was the rapid establishment of steep thermal stratification in spring (spring mixing persisted only about 5 d in KWK16 in 2008; Fig. 5). The deeper water masses were rapidly isolated from the atmosphere, with anoxia leading to anaerobic metabolism. A stable thermocline in a 2- or 3-m deep waterbody with a stability index (N) of 0.04 to 0.1 s^{-1} was unexpected at these latitudes but was explained by the strong attenuation of shortwave solar radiation in these waterbodies, in combination with their short wind fetch.

As a result of the stratification, both CO_2 and CH_4 increased at depth to attain values up to 836 μmol L^{-1} of CO_2 and 127 μmol L^{-1} of CH_4 (at 2-m depth in the anoxic

water of pond KWK21). Gas buildup in bottom waters is likely a consequence of the physical isolation of this water mass, while increasing concentrations toward sediments vary proportionally with the sediment area : water volume ratio of each water layer. Such high dissolved gas concentrations have also been reported in thaw lakes and ponds of the Kolyma River Lowland region in Siberia (Semiletov et al. 1996). With the sediment–water CH_4 flux obtained by Huttunen et al. (2006) in a small boreal lake (27 mg m^{-2} d^{-1}), the time required to reach the hypolimnetic CH_4 concentration measured in pond KWK23 (1.97 mg CH_4 L^{-1} averaged from the two depths where data were recorded; Fig. 4) was estimated to 110 d (estimated hypolimnion volume = 427 m^3 and sediment area = 285 m^2). This pond was likely stratified only for about 40 d prior to sampling (based on the stratification regime established in the similar pond KWK16). However, if these ponds do not entirely mix in spring, concentrations may remain higher, thus allowing for greater accumulation over time and supporting the flux calculations above. The increased specific conductivity in the bottom waters of some ponds also suggests incomplete mixing. Differences in the nature of the available organic matter and microbial communities (e.g., the balance between methanogens and methanotrophs) will also affect gas accumulation rates.

In subarctic pond KWK2, the combination of surface meteorology and time series measurements of gas concentrations allowed insights into the combined effects of biological processes and drivers of vertical mixing on gas fluxes. Concentrations of CO_2 and CH_4 increased in the upper water column in response to cooling at the surface, which likely drove the convective entrainment of these gases from deeper in the water column. Cold fronts are most likely to cause increases in fluxes, which doubled in the present study during such events. The time series temperature data from KWK16 (Fig. 5) indicate cooling events occurred four to six times per month in the summer and usually persist for several days. Summer mixing events will be likely in shallower ponds, especially the least turbid and humic ones. These high-resolution data point to methods to improve the accuracy of predicting changes in fluxes with climate warming. Gas ventilation would occur periodically in cool summers but could potentially be delayed until autumn in warm summers since the water column is more stable. Water column dynamics just prior to ice-on would determine whether these gases are vented to the atmosphere or sequestered until next spring, with increased opportunity for ongoing transformations (e.g., consumption of CH_4 by methanotrophs). The remarkable and persistent stability of the subarctic thaw ponds indicates that considerable concentrations of GHG may be vented during fall overturn. This autumnal venting from subarctic stratified ponds could be linked to the late-autumn shoulder consistently observed in the seasonal cycles of atmospheric methane at high latitudes (Dlugokencky et al. 1994). Thus, sampling efforts should also be made at this time of the year, as well as during the spring liberation of gases accumulated under the ice (Michmerhuizen et al. 1996). The accentuation of thermal stratification (faster in spring, more stable in summer) expected as a consequence of global warming (Jankowski et al. 2006) will also affect seasonal variations in GHG evasion.

Heterotrophic thaw ponds—The subarctic thaw ponds were relatively rich in organic matter and in phosphorus, but their low light environment would favor heterotrophy over phototrophy. The ponds indeed harbored abundant bacteria (Table 1) relative to concentrations found in temperate lakes (e.g., 1.7 to 5.9 $\times$ 10^6 mL^{-1}, n = 14; del Giorgio et al. 1997). Therefore, net heterotrophy and the observed large CO_2 evasion were to be expected in these ponds. On the other hand, arctic ponds were often net autotrophic (mostly polygon ponds; Fig. 3). The arctic ponds that were net heterotrophic (runnel ponds) presented signs of recent peat erosion, higher DOC contents, and higher aromaticity (a_{320} : DOC). Climate warming can lead to increased peat erosion in this type of landscape with the formation of abundant runnel ponds, resulting in the liberation of soil organic carbon and its respiration to the atmosphere (the highest C fluxes were measured in runnel ponds). In contrast, the polygon ponds colonized by benthic cyanobacterial mats are a carbon sink (a CO_2 sink, but not a CH_4 sink) and are vulnerable to climate warming, with their water draining either through fissures that form across the polygons or during periods of reduced precipitation : evaporation ratios (Fig. 2f). It will be essential to monitor multiple successional stages in these ecosystems as climate warms to fully estimate their role in GHG production and global feedback effects.

Greenhouse gas fluxes—In the ponds where chamber flux measurements were taken several times during the day (one subarctic and five arctic ponds), variations were high (coefficients of variation of 37% to 210%), with values always higher when taken earlier in the day (not shown). This suggests that nocturnal mixing brought more gas to the air–water interface (Crill et al. 1988). Therefore, the time of sampling is a source of variability that needs to be considered. Our estimates of fluxes are limited by several factors. First, wind was estimated from a relatively distant climate station (but within 500 m in most cases), and local topographic variations, although slight, may have caused errors in our estimates of flux rates. The difference observed between fluxes obtained with a floating chamber and with the conservative wind-based model of Cole and Caraco (1998; Table 3; on average 2.5 times lower when using the chamber) is likely the result of several factors. The wind was measured at 10 m aboveground, while the model was developed for lakes of longer fetch length where shore topography does not affect the boundary layer. At the present study sites, pond area was sometimes only a few square meters, and the local topography (at arctic site, Fig. 2e) and thick surrounding vegetation (at subarctic site, Fig. 2b) may have led to lower shear stresses than would have occurred in the larger waterbodies where most of the empirical studies have been conducted to develop equations for the gas transfer coefficient (Kwan and Taylor 1994). Consequently, gas exchange may be lower than computed.

Surface films of surfactants (Banerjee and MacIntyre 2004), abundant in those small, humic, and microbially active thaw ponds, could also act to reduce gas exchanges through the interface, a factor that is not considered in wind-based models. Finally, chamber deployment has been shown to enhance gas transfer through disturbance of the surface boundary layer (Matthews et al. 2003) and cannot be completely excluded in the present study.

The highest CO_2 flux measured was in the Arctic for a humic pond (BYL38; DOC = 20.8 mg L^{-1}) that had apparently been formed by erosion of soils on the side of a moraine deposit (arrow in Fig. 2d). The flux measured with the floating chamber reached 909 mg C m^{-2} d^{-1} (at noon; the value given in Table 3 for BYL38 is an average of three separate measurements). This result suggests that newly formed runnel ponds may release large amounts of carbon at the beginning of the erosional cycle, followed by reduced evasions as labile carbon is used up.

To compare the CO_2 fluxes obtained in the present study with literature values, we extrapolated our instantaneous flux values to provide a first estimate of annual rates. Annual CO_2 fluxes ranged from 39 to 273 g C m^{-2} in the subarctic ponds (average of 122 g C m^{-2} yr^{-1}, $n = 12$). These values have a high level of uncertainty given the diel and seasonal variations; however, they are likely to be underestimates since they were calculated using surface water concentrations of CO_2 and they neglect evasion during fall cooling as well as changes under the ice. Also, as demonstrated with the application of three models to compute gas transfer coefficients, the wind-based model (Cole and Caraco 1998), which was used to calculate fluxes in the pond data series, is the most conservative. Given these caveats, the CO_2 fluxes estimated for subarctic ponds in the present study fall within the range reported by Kortelainen et al. (2006) for small boreal lakes (average of 102 g C m^{-2} yr^{-1} for lakes smaller than 0.1 km^2). They are higher than those estimated from a large series of boreal lakes in Sweden (0.63 to 5 g C m^{-2} yr^{-1}; Algesten et al. 2003) or from arctic lakes and rivers in Alaska (average of 24 g C m^{-2} y^{-1}; Kling et al. 1992) but much lower than those values reported for wetland ponds in the Hudson Bay lowland (1350–4015 g C m^{-2} yr^{-1}, also derived from daily fluxes extrapolated to the full year; Hamilton et al. 1994). This simple comparison demonstrates the need for improved regional and temporal coverage of GHG flux measurements. Further studies are also needed to verify the 40% increase in fluxes obtained when using gas transfer coefficients based on eddy covariance data (Fig. 9), and, as noted above, to address the role of surfactants and the changes in the characteristics of the atmospheric boundary layer over small waterbodies and the predicted gas transfer coefficients.

The area covered by thaw ponds in northeastern Canada is unknown at this stage, but it was estimated to cover 8–12% of the landscape in Hudson Bay lowlands (Hamilton et al. 1994) and 15–40% in the arctic coastal plain of northern Alaska (Hinkel et al. 2005). Since Canada has 4 million km^2 occupied by permafrost and under the assumption that 5% of this area is occupied by thaw ponds involving soil erosion (thermokarst), a global carbon evasion from Canadian thaw ponds can be estimated. Using the average surface flux values from subarctic and arctic ponds (2007 data series, excluding the polygon ponds with cyanobacterial mats), we obtain annual diffusive flux from Canadian thaw ponds of 95 Tg CO_2 and 1.0 Tg CH_4. Current estimates of CO_2 evasion from lakes range from 257 to 550 Tg CO_2 yr^{-1} (Cole et al. 2007), an estimate that does not include thaw ponds as studied here. In general, methane losses by ebullition exceed diffusive fluxes. For example, Walter at al. (2006) estimated that molecular diffusion of methane was 5% of total emissions from Siberian thermokarst lakes. The present study CH_4 fluxes were indeed lower than what was measured in other thermokarst lakes and ponds (Walter et al. 2006; Wickland et al. 2006; Blodau et al. 2008) or permafrost-influenced aquatic systems (Nakano et al. 2000; Ström and Christensen 2007) but close to estimates based on the eddy covariance method in polygonal tundra (similar to the present study arctic site; Sachs et al. 2008). However, ebullition in Canadian thaw ponds is possibly lower than ebullition from thick yedoma organic sediments beneath Siberian thaw lakes (Walter et al. 2008). Therefore, even though this estimation of annual methane flux from Canadian thaw ponds is possibly underestimated, it is comparable to the global annual evasion of 3.8 Tg CH_4 calculated for Northern Siberian thaw lakes and significant in comparison to the 6–40 Tg CH_4 emitted annually by northern wetlands (Walter et al. 2006). Moreover, in these annual estimations, we assumed a constant evasion of gases at summer rates (surface water fluxes were only including the contribution by benthic respiration from the littoral zone comprised in the mixing layer) and did not consider the accumulation of gases in deeper strata of the water column during the summer (subsidized by anoxic respiration below the mixing layer). Using the gas profile obtained in one stratified subarctic thaw pond (KWK23, Fig. 4) and a trapezoidal integration of the gases trapped below the mixed layer (< 0.75 m), we estimate that the autumnal mixing period could release to the atmosphere more than two times the CH_4 evasion calculated for continuous loss over 365 d using surface water July rate. On the other hand, the shallower arctic ponds are frozen to the bottom for a large part of the year and therefore most likely not releasing greenhouse gases during this period.

Indicators of gas content—Efforts have been made to predict CO_2 from DOC in lake systems. Methods to estimate past DOC using a paleolimnological approach (Pienitz and Vincent 2000) or current DOC using remote sensing (Kutser et al. 2005) would help us to scale up our predictions of CO_2 concentrations or evasion rates in time and space. However, contrasting results have been reported on the predictive strength of DOC (as bulk measure of DOM) for the estimation of CO_2 in lake waters, with, for example, significant correlations found in boreal lakes (Sobek et al. 2005) and nonsignificant correlations in small (Kortelainen et al. 2006) or large boreal lakes (Rantakari and Kortelainen 2005) and in northern temperate lakes (del Giorgio et al. 1997). In the present study, when both sites and years were combined, we did not obtain a significant correlation between CO_2 and DOC, but the relation became significant when the

subarctic ponds were considered alone (although r remained low at 0.411, $p = 0.007$). The differing trends revealed by these studies may result from the difficulty to adequately describe the huge variability in microbial availability and photochemical reactivity of DOM in aquatic systems simply using DOC. It could also be linked to more complex interactions between DOM, food web structure, and sedimentation carbon losses (Flanagan et al. 2006).

Other DOM descriptors, such as the absorbance and fluorescence properties, were used more successfully than DOC to explain the differing rates of microbial and photochemical degradation (Stedmon and Markager 2005). We obtained a better relationship between dissolved CO_2 and the chromophoric portion of DOM (i.e., the absorption coefficient). Additionally, we observed a correlation between CO_2 and a_{320} : DOC. These results suggest that (1) a significant part of the CO_2 originates from DOM photolysis since it is related to DOM chromophoricity (Opsahl and Benner 1998); (2) the chromophoric components of DOM (generally considered of a higher molecular weight) were used more successfully by the microbial community (as found in marine waters by Amon and Benner 1994); or (3) DOM exerts an indirect effect on CO_2 through its effect on temperature, light availability, and water column structure. The chromophoric properties of DOM are prevalent in all of these relationships. Overall, these empirical relationships have a relatively low predictive power, and the models developed for one ecosystem type may be poorly applicable to other systems. For example, CO_2 concentrations estimated from a model developed on 176 boreal lakes by Algesten et al. (2003, using TOC equal to DOC) were correlated with CO_2 concentrations measured in the present study for subarctic ponds ($r = 0.429$ and $p = 0.005$), but the values differ on average by 28%.

Thawing of permafrost has been identified as one of the five most vulnerable carbon pools that can have drastic consequences for atmospheric carbon through positive feedback mechanisms (Gruber et al. 2004). However, the size of this high-latitude pool, the processes affecting it, and the timescale of change involved are yet to be quantified (Schuur et al. 2008). Climate change not only has the potential to mobilize a large pool of stored carbon, it will also affect water temperature, with direct effects on microbial growth and respiration. Perhaps most importantly, climate change will affect the duration of ice cover and the precipitation regime, hence the light and stratification patterns and the hypolimnetic oxygen concentrations, which all have consequences on GHG evasion rates. With a total coverage estimated at about 4.6 million km^2 (Downing et al. 2006), the great abundance of small lakes and ponds combined with their high biogeochemical activities imply that they play a significant role in the global carbon budget and should be incorporated in climate change projections. This is especially the case for permafrost thaw ponds, which account for a vast surface area and lie on melting, carbon-rich soils. Though most lakes and ponds represent net sources of GHG to the atmosphere, processes such as methanotrophy and primary production at certain sites can reduce or even reverse the GHG fluxes. Changes in stratification dynamics will further influence the likelihood of sequestration vs. gas evasion. These limnological sources of variability in gas exchange will require close attention to fully assess GHG efflux and extent of climate feedback in the rapidly warming polar regions.

Acknowledgments

We thank M.-È. Bédard, F. Bouchard, J. Breton, T. Harding, M.-J. Martineau, N. Rolland, A. Rouillard, M. Rousseau, D. Sarrazin, C. Vallières, and S. Watanabe for their essential support in the field and laboratory; G. Gauthier for support at the Bylot Island field station of the Centre d'études nordiques; M. Allard, Y. Prairie, J.-L. Fréchette, and V. St. Louis for their helpful comments and advice; two anonymous reviewers for their insightful suggestions; L. Marcoux for drafting the map; and the Fonds québécois de la recherche sur la nature et les technologies, Natural Sciences and Engineering Research Council of Canada, ArcticNet, Polar Continental Shelf Project (contribution 02409), Indian and Northern Affairs Canada, Parks Canada, International Polar Year, Centre d'études nordiques, and U.S. National Science Foundation grants DEB-0640953 and ARC-0714085 for logistic and financial support.

References

Åkerman, H. J., and B. Malmström. 1986. Permafrost mounds in the Abisko area, Northern Sweden. Geogr. Ann. **68:** 155–165.

Algesten, G., S. Sobek, A.-K. Bergström, A. Ågren, L. J. Tranvik, and M. Jansson. 2003. Role of lakes for organic carbon cycling in the boreal zone. Glob. Change Biol. **10:** 141–147.

Amon, R. M. W., and R. Benner. 1994. Rapid cycling of high-molecular-weight dissolved organic matter in the ocean. Nature **369:** 549–552.

Banerjee, S., and S. MacIntyre. 2004. The air-water interface: Turbulence and scalar exchange, p. 181–237. *In* J. Grue, P. L. F. Liu and G. K. Pedersen [eds.], Advances in coastal and ocean engineering. World Scientific.

Bastien, J., J.-L. Fréchette, and R. H. Hesslein. 2008. Continuous greenhouse gas monitoring system—operating manual. Report prepared by Environnement Illimité Inc. for Manitoba Hydro and Hydro-Québec.

Bastviken, D., J. J. Cole, M. L. Pace, and M. C. V. De Bogert. 2008. Fates of methane from different lake habitats: Connecting whole-lake budgets and CH_4 emissions. J. Geophys. Res. Biogeosci. **113:** G02024, doi:10.1029/2007JG000608.

Blodau, C., and others. 2008. A snapshot of CO_2 and CH_4 evolution in a thermokarst pond near Igarka, northern Siberia. J. Geophys. Res. Biogeosci. **113:** G03023, doi: 10.1029/2007JG000652.

Bonilla, S., V. Villeneuve, and W. F. Vincent. 2005. Benthic and planktonic algal communities in a high Arctic lake: Pigment structure and contrasting responses to nutrient enrichment. J. Phycol. **41:** 1120–1130.

Breton, J., C. Vallières, and I. Laurion. 2009. Limnological properties of permafrost thaw ponds in northeastern Canada. Can. J. Fish. Aquat. Sci. **66:** 1635–1648.

Carignan, R. 1998. Automated determination of carbon dioxide, oxygen, and nitrogen partial pressures in surface waters. Limnol. Oceanogr. **43:** 969–975.

Chapin, F. S., and others. 2000. Arctic and boreal ecosystems of western North America as components of the climate system. Glob. Change Biol. **6:** 211–223.

Cole, J. J., and N. F. Caraco. 1998. Atmospheric exchange of carbon dioxide in a low-wind oligotrophic lake measured by the addition of SF6. Limnol. Oceanogr. **43:** 647–656.

———, and others. 2007. Plumbing the global carbon cycle: Integrating inland waters into the terrestrial carbon budget. Ecosystems **10:** 171–184.

Crill, P., and others. 1988. Tropospheric methane from an Amazon floodplain lake. J. Geophys. Res. **93:** 1564–1570.

del Giorgio, P. A., J. J. Cole, N. F. Caraco, and R. H. Peters. 1999. Linking planktonic biomass and metabolism to net gas fluxes in northern temperate lakes. Ecology **80:** 1422–1431.

———, ———, and A. Cimbleris. 1997. Respiration rates in bacteria exceed phytoplankton production in unproductive aquatic systems. Nature **385:** 148–151.

Dlugokencky, E. J., L. P. Steele, P. M. Lang, and K. A. Masarie. 1994. The growth rate and distribution of atmospheric methane. J. Geophys. Res. **99:** 17021–17043.

Downing, J. A., and others. 2006. The global abundance and size distribution of lakes, ponds, and impoundments. Limnol. Oceanogr. **51:** 2388–2397.

Flanagan, K. M., E. McCauley, and F. Wrona. 2006. Freshwater food webs control carbon dioxide saturation through sedimentation. Glob. Change Biol. **12:** 644–651.

Fortier, D., and M. Allard. 2004. Late Holocene syngenetic ice-wedge polygons development, Bylot Island, Canadian Arctic archipelago. Can. J. Earth Sci. **41:** 997–1012.

Granéli, W., M. Lindell, and L. Tranvik. 1996. Photo-oxidative production of dissolved inorganic carbon in lakes of different humic content. Limnol. Oceanogr. **41:** 698–706.

Gruber, N., and others. 2004. The vulnerability of the carbon cycle in the 21st century: An assessment of carbon-climate-human interactions, p. 45–76. *In*: C. B. Field and M. R. Raupach [eds.], The Global Carbon Cycle: Integrating Humans, Climate, and the Natural World. Island Press.

Gundersen, K., G. Bratbak, and M. Heldal. 1996. Factors influencing the loss of bacteria in preserved seawater samples. Mar. Ecol. Prog. Ser. **137:** 305–310.

Hamilton, J. D., C. A. Kelly, J. W. M. Rudd, R. H. Hesslein, and N. T. Roulet. 1994. Flux to the atmosphere of CH_4 and CO_2 from wetland ponds on the Hudson-Bay Lowlands (HBLs). J. Geophys. Res. Atmos. **99:** 1495–1510.

Hanson, P. C., D. L. Bade, S. R. Carpenter, and T. K. Kratz. 2003. Lake metabolism: Relationships with dissolved organic carbon and phosphorus. Limnol. Oceanogr. **48:** 1112–1119.

Hesslein, R. H., J. W. M. Rudd, C. Kelly, P. Ramlal, and K. A. Hallard. 1990. Carbon dioxide pressure in surface waters of Canadian lakes, p. 413–431. *In* S. C. Wilhelms and J. S. Gulliver [eds.], Air-water mass transfer. American Society of Civil Engineers.

Hinkel, K. M., R. C. Frohn, F. E. Nelson, W. R. Eisner, and R. A. Beck. 2005. Morphometric and spatial analysis of thaw lakes and drained thaw lake basins in the western arctic coastal plain. Permafrost Periglac. Proc. **16:** 327–341.

Huttunen, J. T., T. S. Väisänen, S. K. Hellsten, and P. J. Martikainen. 2006. Methane fluxes at the sediment-water interface in some boreal lakes and reservoirs. Boreal Environ. Res. **11:** 27–34.

Imberger, J. 1985. The diurnal mixed layer. Limnol. Oceanogr. **30:** 737–770.

International Panel on Climate Change (IPCC). 2007. The physical science basis: summary for policymakers. Fourth Assessment Report. Cambridge University Press.

Jankowski, T., D. M. Livingstone, H. Bührer, R. Forster, and P. Niederhauser. 2006. Consequences of the 2003 European heat wave for lake temperature profiles, thermal stability, and hypolimnetic oxygen depletion: Implications for a warmer world. Limnol. Oceanogr. **51:** 815–819.

Jonsson, A., J. Aberg, A. Lindroth, and M. Jansson. 2008. Gas transfer rate and CO_2 flux between an unproductive lake and the atmosphere in northern Sweden. J. Geophys. Res. **113:** G04006, doi:10.1029/2008JG000688.

———, M. Meili, A.-K. Bergström, and M. Jansson. 2001. Whole-lake mineralization of allochthonous organic carbon in a large humic lake (Örträsket, N. Sweden). Limnol. Oceanogr. **46:** 1691–1700.

Kankaala, G., J. Huotari, E. Peltomaa, T. Saloranta, and A. Ojala. 2006. Methanotrophic activity in relation to methane efflux and total heterotrophic bacterial production in a stratified, humic, boreal lake. Limnol. Oceanogr. **51:** 1195–1204.

Kling, G. W., G. W. Kipphut, and M. C. Miller. 1992. The flux of CO_2 and CH_4 from lakes and rivers in arctic Alaska. Hydrobiologia **240:** 23–36.

Kortelainen, P., and others. 2006. Sediment respiration and lake trophic state are important predictors of large CO_2 evasion from small boreal lakes. Glob. Change Biol. **12:** 1554–1567.

Kutser, T., D. Pierson, L. Tranvik, A. Reinart, S. Sobek, and K. Kallio. 2005. Using satellite remote sensing to estimate the colored dissolved organic matter absorption coefficient in lakes. Ecosystems **8:** 709–720.

Kwan, J., and P. A. Taylor. 1994. On gas fluxes from small lakes and ponds. Boundary-Layer Meteorol. **68:** 339–356.

MacIntyre, S., J. P. Fram, P. J. Kushner, W. J. O'Brien, J. E. Hobbie, and G. W. Kling. 2009. Climate-related variations in mixing dynamics in an Alaskan arctic lake. Limnol. Oceanogr. **54:** 2401–2417.

———, J. R. Romero, and G. W. Kling. 2002. Spatial-temporal variability in mixed layer deepening and lateral advection in an embayment of Lake Victoria, East Africa. Limnol. Oceanogr. **47:** 656–671.

———, R. Wanninkhof, and J. P. Chanton. 1995. Trace gas exchange across the air-water interface in freshwater and coastal marine environments, p. 52–97. *In* P. A. Matson and R. C. Harriss [eds.], Biogenic trace gases: Measuring emission from soil and water. Blackwell.

Matthews, C. J. D., V. L. St. Louis, and R. H. Hesslein. 2003. Comparison of three techniques used to measure diffusive gas exchange from sheltered aquatic surfaces. Environ. Sci. Technol. **37:** 772–780.

Michmerhuizen, C. M., R. G. Striegl, and M. E. McDonald. 1996. Potential methane emission from north-temperate lakes following icemelt. Limnol. Oceanogr. **41:** 985–991.

Nakano, T., S. Kuniyoshi, and M. Fukuda. 2000. Temporal variation in methane emission from tundra wetlands in a permafrost area, northeastern Siberia. Atmos. Environ. **34:** 1205–1213.

Obernosterer, I., and R. Benner. 2004. Competition between biological and photochemical processes in the mineralization of dissolved organic carbon. Limnol. Oceanogr. **49:** 117–124.

Opsahl, S., and R. Benner. 1998. Photochemical reactivity of dissolved lignin in river and ocean waters. Limnol. Oceanogr. **43:** 1297–1304.

Pienitz, R., P. T. Doran, and S. F. Lamoureux. 2008. Origin and geomorphology of lakes in the polar regions, p. 25–41. *In* W. F. Vincent and J. Laybourn-Parry [eds.], Polar lakes and rivers—limnology of arctic and antarctic aquatic ecosystems. Oxford Univ. Press.

———, AND W. F. VINCENT. 2000. Effect of climate change relative to ozone depletion on UV exposure in subarctic lakes. Nature **404:** 484–487.

RANTAKARI, M., AND P. KORTELAINEN. 2005. Interannual variation and climatic regulation of the CO_2 emission from large boreal lakes. Glob. Change Biol. **11:** 1368–1380.

SACHS, T., C. WILLE, J. BOIKE, AND L. KUTZBACH. 2008. Environmental controls on ecosystem-scale CH_4 emission from polygonal tundra in the Lena River Delta, Siberia. J. Geophys. Res. Biogeosci. **113:** G00A03, doi:10.1029/2007JG 000505.

SCHUUR, E. A. G., AND OTHERS. 2008. Vulnerability of permafrost carbon to climate change: Implications for the global carbon cycle. BioScience **58:** 701–714.

SEMILETOV, I. P., I. I. PIPKO, N. YA. PIVOVAROV, V. V. POPOV, S. A. ZIMOV, YU. V. VOROPAEV, AND S. P. DAVIODOV. 1996. Atmospheric carbon emission from North Asian Lakes: A factor of global significance. Atmos. Environ. **30:** 1657–1671.

SOBEK, S., L. J. TRANVIK, AND J. J. COLE. 2005. Temperature independence of carbon dioxide supersaturation in global lakes. Glob. Biogeochem. Cycles **19:** GB 2003, doi:10.1029/ 2004GB002264.

STAINTON, M., M. J. CAPEL, AND A. ARMSTRONG. 1977. The chemical analysis of freshwater. Can. Fish. Mar. Serv. Misc. Spec. Publ., 25.

STEDMON, C. A., AND S. MARKAGER. 2005. Tracing the production and degradation of autochthonous fractions of dissolved organic matter by fluorescence analysis. Limnol. Oceanogr. **50:** 1415–1426.

STRIEGL, R. G., AND C. M. MICHMERHUIZEN. 1998. Hydrologic influence on methane and carbon dioxide dynamics at two north-central Minnesota lakes. Limnol. Oceanogr. **43:** 1519–1529.

STRÖM, L., AND T. R. CHRISTENSEN. 2007. Below ground carbon turnover and greenhouse gas exchanges in a sub-arctic wetland. Soil Biol. Biochem. **39:** 1689–1698.

VÉZINA, S., AND W. F. VINCENT. 1997. Arctic cyanobacteria and limnological properties of their environment: Bylot Island, Northwest territories, Canada (73 Degrees N, 80 Degrees W). Polar Biol. **17:** 523–534.

VINCENT, W. F. 2009. Effects of climate change on lakes, p. 55–60. *In* G. Likens [ed.], Encyclopedia of inland waters, vol. 3. Elsevier.

WALTER, K. M., J. P. CHANTON, F. S. CHAPIN III, E. A. G. SCHUUR, AND S. A. ZIMOV. 2008. Methane production and bubble emissions from arctic lakes: Isotopic implications for source pathways and ages. J. Geophys. Res. **113:** G00A08, doi:10.1029/2007JG000569.

———, M. E. EDWARDS, G. GROSSE, S. A. ZIMOV, AND F. S. CHAPIN, III. 2007. Thermokarst lakes as a source of atmospheric CH_4 during the last deglaciation. Science **318:** 633–636.

———, S. A. ZIMOV, J. P. CHANTON, D. VERBYLA, AND F. S. CHAPIN. 2006. Methane bubbling from Siberian thaw lakes as a positive feedback to climate warming. Nature **443:** 71–75.

WICKLAND, K. P., R. G. STRIEGL, J. C. NEFF, AND T. SACHS. 2006. Effects of permafrost melting on CO_2 and CH_4 exchange of a poorly drained black spruce lowland. J. Geophys. Res. Biogeosci. **111:** G02011, doi:10.1029/2005JG000099.

ZAPATA, M., F. RODRIGUEZ, AND J. L. GARRIDO. 2000. Separation of chlorophylls and carotenoids from marine phytoplankton: a new HPLC method using a reversed phase C8 column and pyridine containing mobile phases. Mar. Ecol. Prog. Ser. **195:** 29–45.

ZIMOV, S. A., AND OTHERS. 1997. North Siberian lakes: A methane source fuelled by Pleistocene carbon. Science **277:** 800–802.

Associate editor: Samantha B. Joye

Received: 19 January 2009
Accepted: 19 August 2009
Amended: 09 September 2009